

Planar Pentacoordinate Aluminium and Gallium Atoms

Famaz Yashmin

Cotton University

Amlan J. Kalita

Cotton University

Ritam R. Borah

Cotton University

Indrani Baruah

Cotton University

Rinu P. Deka

Cotton University

Ankur K. Guha (✉ ankurkantiguha@gmail.com)

Cotton University

Research Article

Keywords:

Posted Date: March 21st, 2022

DOI: <https://doi.org/10.21203/rs.3.rs-1449900/v1>

License:   This work is licensed under a Creative Commons Attribution 4.0 International License.

[Read Full License](#)

Abstract

Planar hypercoordinate structures are gaining immense attention due to the shift from common paradigm. Herein, our high level *ab initio* calculations predict that planar pentacoordinate aluminium and gallium centres in $\text{Cu}_5\text{Al}^{2+}$ and $\text{Cu}_5\text{Ga}^{2+}$ clusters are global minima in their singlet ground states. These clusters are thermodynamically and kinetically very stable. Detailed electronic structure analyses reveal the presence of both σ and π aromaticity which is the driving force for the stability of the planar form.

Introduction

Introducing new chemical structures is one of the most important goals in chemistry. Challenging the known dogma of chemical structure has always been fascinating in chemical community. One such example of rule breaking structure is the case of planar tetracoordinate carbon (ptC) which was first convincingly proposed in 1968 to exist in planar D_{4h} transition states between tetrahedral enantiomers of simple substituted methane [1]. This observation led Hoffmann, Alder, and Wilcox in 1970 to explore the electronic feature for the stabilization of such ptCs by using molecular orbital theory [2]. However, *ab initio* study revealed that isolation of planar methane is impossible as the energy difference between the planar and tetrahedral form is 130 kcal/mol [3]. The first global minimum ptCs were predicted in 1976 on some Li-substituted ptC molecules and 1,1-dilithiocyclopropane and 3,3-dilithio-cyclopropene molecules [4]. The first experimental evidence of ptC came in the year 1977 [5]. Since then many planar penta- (ppC), hexa- (phC) and hepta-coordinate (p7C) carbon were computationally explored [6-15]. For example, in 2008, the first ppC, CAI_5^+ was experimentally characterized and theoretically found to be global minima [14]. Similarly, the first phC, B_6C^{2-} was proposed by Schleyer and co-workers [11], however, the latter study revealed that carbon avoids planar hypercoordination [12]. The true global minimum containing a phC was recently proposed [15] which contain a planar hexacoordinate carbon atom surrounded by ligands with half covalent and half ionic bonding. Such achievements of novel hypercoordinate carbon (hpC) molecules have created a new dogma in present day chemistry that highest coordination number of carbon is no longer four.

These studies have also inspired the quest for other systems containing planar hypercoordinate main group elements such as group 13 elements. The first molecule containing planar hexacoordinate boron (phB) was predicted in 1991 [16] which triggered further examples of hypercoordinate boron [16-26]. Zhai *et al* [19] reported experimental and theoretical evidence of perfectly planar B_8^- and B_9^- anions clusters with hepta and octa-coordinate boron atom. Theoretical study by Yu *et al* [25] revealed that B_6H_5^+ cation is aromatic with a planar pentacoordinate boron (ppB) centre. We have also recently reported a phB species, BBe_6H_6^+ cluster featuring double aromaticity [26]. Unlike B, its heavier analogues (Al and Ga) received little attention in the realm of planar hypercoordination. Schleyer and co-workers had shown that there is a dramatic drop in the energy of lowest unoccupied molecular orbital (LUMO) upon planarization of AlH_4^- [27]. Experimental realization of ptAl species has been reported [28-29]. Averkiev and co-workers

[30] have made an in silico prediction of planar nonacoordinate aluminum centre, AlB_9 , based on previously proved doubly aromatic boron clusters [19]. A cluster containing a phAl in the global minimum form of Al_4C_6 cluster was also reported [31]. Similarly, recent theoretical study has also reported a thermodynamically and kinetically stable phGa species [32]. Despite of these achievements, reports on planar pentacoordinate Al and Ga centres (ppAl and ppGa) in isolated clusters are extremely rare. Herein, we report the global minimum of ppAl and ppGa centres in isolated binary clusters, Cu_5Al^{2+} and Cu_5Ga^{2+} . The proposed ppAl and ppGa clusters are found to be thermodynamically and kinetically stable and possess double aromaticity.

Computational Details

In order to explore systematically the potential energy surface of the title compound, ABCluster code [33–34] in combination with M06-2X/TZVP level [35] has been adopted which produced 30 stationary points. Full optimization of the low lying isomers was done using M06-2X/def2-TZVP level. The energies were then refined by running single point calculations at CCSD(T)/def2-TZVP level of theory on M06-2X optimized geometries. Vibrational harmonic frequency calculations were also performed at M06-2X/def2-TZVP level to confirm that the structures are true minima. All these calculations were performed using Gaussian16 suite of programs [36]. The electronic structure of the molecules were analyzed using natural bond orbital (NBO) [37] calculations at M06-2X/def2-TZV level. ETS-NOCV analysis were performed at M06-2X/def2-TZVP level considering cationic Al and Ga (triplet) and triplet Cu_5^+ as ΔE_{orb} for these fragmentation is the least and hence the best choice [38]. In addition, adaptive natural density partitioning (AdNDP) [39], quantum theory of atoms in molecules (QTAIM) [40] and electron localization function (ELF) [41] were also analyzed at M06-2X/def2-TZV level using Multiwfn program code [42]. To quantify the aromaticity, nucleus independent chemical shift calculations (NICS) [43] were performed by placing a ghost atom (symbol Bq) at the geometric mean of the Cu-Al-Cu and Cu-Ga-Cu rings and with an incremental distance of 0.2 Å above the ring upto a distance of 2 Å.

Results And Discussion

Figure 1 shows the optimized geometries of the global minima of Cu_5Al^{2+} and Cu_5Ga^{2+} along with their low energy isomers calculated at CCSD(T)/def2-TZVP//M06-2X/def2-TZVP level. The global minima of Cu_5Al^{2+} (**1A**) and Cu_5Ga^{2+} (**1G**) clusters feature D_{5h} symmetry in their singlet spin ground states. The Cu-Al distance in **1A** is 2.481 Å (Wiberg bond index is 0.512) while the Cu-Cu distance is 2.917 Å (WIB is 0.052). Similarly, the Cu-Ga distance in **1G** is 2.500 Å (WIB is 0.492) and Cu-Cu distances are in the range 2.932–2.942 Å (WIBs are in the range (0.045–0.048)). The computed natural charges using NBO method reveals a negative charge of -1.28e and -1.37e for the central Al and Ga atoms respectively. This implies a significant amount of charge donation from the Cu_5 unit to the central Al and Ga atoms.

We then turned our attention to investigate the electronic structure of the ppAl and ppGa structures. For this, we used adaptive natural density partitioning (AdNDP) scheme [39]. AdNDP partitions the electron

density in n-centre n-electron bonds and is very helpful in understanding the presence of multicentre bonds [39]. Figure 2 shows the bonds recovered using AdNDP analysis of $\text{Cu}_5\text{Al}^{2+}$ cluster as a representative case. There is formation of five 2c-2e, 3c-2e and 4c-2e Cu-Al σ bonds. In addition, there is a formation of a 6c-2e Cu-Al π bond. This π orbital is delocalized and may be responsible for π aromaticity in the cluster. AdNDP analysis could also locate three 6c-2e Cu-Al σ bonds which may result in σ -aromaticity in the ring. The nature of Cu-Al and Cu-Ga bonds have been further analyzed within the realm of quantum theory of atoms in molecules (QTAIM) [40] and electron localization function (ELF) [41]. The Cu-Al and Cu-Ga bonds are characterized by significant presence of electron density ρ (0.04 a.u) at the bond critical points, negative value of Laplacian of electron density $\nabla^2\rho$, negative value of local electronic energy density, $H(r)$ and significant value of electron localization function (ELF) (Table 1). All these topological parameters refer to covalent character of the Cu-Al and Cu-Ga bonds. The Laplacian plot of electron density and electron localization function (Fig. 3) in the molecular plane clearly reveals significant electron delocalization.

Table 1

Electron density (ρ) at the bond critical points, Laplacian of electron density ($\nabla^2\rho$), total electronic energy density ($H(r)$) and natural charges (q) in |e|. All other values are in a.u.

Molecule	bcp	ρ	$\nabla^2\rho$	$H(r)$	ELF	qAl	qGa	qCu
$\text{Cu}_5\text{Al}^{2+}$	Cu-Al bcp	0.048	-0.022	-0.012	0.67	-1.28		0.65
$\text{Cu}_5\text{Ga}^{2+}$	Cu-Ga bcp	0.038	0.027	-0.012	0.38		-1.37	0.46

Again, to further quantify the strength of Cu-Al and Cu-B bonds, we carried out extended-transition state method for energy decomposition analysis combined with natural orbital of chemical valence (ETS-NOCV) (Fig. 4) [38]. The ETS-NOCV analysis suggests significant covalent nature of Cu-Al and Cu-Ga bonds. The NOCV pair densities were generated by considering two fragments, Al^+ and Ga^+ in triplet state and Cu_5^+ in triplet state. Table S1 provides the numerical results of ETS-NOCV considering Al, Ga and Cu_5 in different charges and electronic states as interacting fragments. Inspection of the relative size of ΔE_{orb} value reveal that the most reasonable fragmentation scheme is Al and Ga in cationic triplet state with ns^1np^1 forming an electron-sharing π bond with the triplet Cu_5^+ state. This fragmentation provides the best description of ETS-NOCV as these fragments give the lowest ΔE_{orb} value. Apart from ${}^3\text{Al}^+ / {}^3\text{Ga}^+ \rightarrow {}^3\text{Cu}_5^+$ σ -donation, a significant amount of ${}^3\text{Cu}_5^+ \rightarrow {}^3\text{Al}^+ / {}^3\text{Ga}^+$ σ -backdonation is also evident in the analysis. In addition, a significant amount of ${}^3\text{Cu}_5^+ \rightarrow {}^3\text{Al}^+ / {}^3\text{Ga}^+$ π -donation is also found. These ${}^3\text{Cu}_5^+ \rightarrow {}^3\text{Al}^+ / {}^3\text{Ga}^+$ donations accounts for the negative charges at central Al and Ga atoms.

For the quantify the aromaticity in the ppAl and ppGa global minima, we have performed nucleus independent chemical shift (NICS) [43] calculations. NICS calculations are shown in Fig. 5. NICS profile for ppGa is shown in Figure S1, supporting information. Significant negative values of the NICS_{ZZ} are

found in the molecular plane and upto 2 Å above the molecular plane. This suggests the presence of both σ and π aromatic character in the cluster. Dissected canonical molecular orbital-NICS (CMO-NICS) also confirmed the presence of significant contribution from σ orbitals and π orbital. Thus, the cluster possesses double aromaticity.

To investigate the dynamic stability of these clusters, we performed Born-Oppenheimer molecular dynamics (BOMD) simulations for a time period of 25 ps (Fig. 6). with a step size of 0.5 fs from the equilibrium global minimum structure with random velocities assigned to the atoms according to a Maxwell-Boltzmann distribution for one temperature, and then normalized so that the net moment for the entire system is zero. The BOMD calculations were performed at room temperature (298 K) and at elevated temperature (450K). Figure 6 reveals that these ppAl and ppGa clusters are stable even at elevated temperature within a time frame of 25 ps.

Conclusion

In summary, quantum chemical calculations predicts the planar petacoordinate Al and Ga centres in $\text{Cu}_5\text{Al}^{2+}$ and $\text{Cu}_5\text{Ga}^{2+}$ are the global minima. These clusters are found to possess double aromaticity which may render stability to the planar form. These planar clusters are thermodynamically and kinetically very stable. Planar pentacoordination of other heavier group 13 elements such as In and Tl are not found. Although, the planar form of $\text{Cu}_5\text{In}^{2+}$ is true local minimum, however, it lies 3.4 kcal/mol higher than the global one (Figure S2). Planar form of $\text{Cu}_5\text{Tl}^{2+}$ is a higher order saddle point on the potential energy surface. Thus, it seems that Cu_5 framework provides the best cavity size and electronic feature to stabilize planar form of Al and Ga as they have similar size. We feel that these clusters may be a suitable target for experimental characterization.

Declarations

ASSOCIATED CONTENT

Data Availability

All the data for this work is available with the corresponding authors on reasonable request.

FUNDING INFORMATION

No funding was provided for this work.

Conflicts of interest

There are no conflicts to declare.

References

1. Monkhorst HJ (1968) *Chem. Commun.* 1111–1112.
2. Hoffmann R, Alder W, Wilcox CF (1970) *J. Am. Chem. Soc.* 92: 4992–4993.
3. Vassilev-Galindo V, Pan S, Donald KJ, Merino G, (2018) *Nat. Rev. Chem.* 2: 0114.
4. Collins JB, Dill JD, Jemmis ED, Apeloig Y, Schleyer PVR, Seeger R, Pople JA, (1976) *J. Am. Chem. Soc.* 98: 5419.
5. Cotton FA, Miller M (1977) *J. Am. Chem. Soc.*, 99: 7886.
6. Yang LM, Ganz E, Chen ZF, Wang ZW, Schleyer PvR (2015) *Angew. Chem., Int. Ed.*, 54: 9468–9501.
7. Sorger K, Schleyer PvR (1995) *J. Mol. Struct.: THEOCHEM*, 338: 317–346.
8. Radom L, Rasmussen DR (1998) *Pure Appl. Chem.*, 70: 1977–1984.
9. Siebert W, Gunale A (1999) *Chem. Soc. Rev.*, 28: 367–371.
10. Keese R (2006) *Chem. Rev.* 106: 4787–4808.
11. Exner K, Schleyer PvR (2000) *Science* 290: 1937.
12. Averkiev BB, Zubarev DY, Wang LM, Huang W, Wang LS, Boldyrev AI (2008) *J. Am. Chem. Soc.* 130: 9248.
13. Guo JC, Feng LY, Barroso J, Merino G, Zhai H (2020) *Chem. Commun.*, 56: 8305–8308.
14. Pei Y, An W, Ito K, Schleyer PvR, Zeng XC (2008) *J. Am. Chem. Soc.*, 130: 10394–10400.
15. Perra LL, Diego L, Yañez O, Inostroza D, Barroso J, Espinal AV, Merino G, Tiznado W (2021) *Angew. Chem. Int. Ed.* DOI: 10.1002/anie.202100940.
16. Bonacic-Koutecky V, Fantucci PJ (1991) *Chem. Rev.*, 91: 1035 and references therein.
17. (a) Gu FL, Yang XM, Tang AC, Jiao HJ, Schleyer PvR (1998) *J. Comput. Chem.*, 19: 203; (b) Rasul R, Olah GA (2001) *Inorg. Chem.* 40: 2453-2456.
18. Gribanova TN, Minyaev RM, Minkin VI (2001) *Mendeleev Commun.*, 11: 169.
19. Zhai HJ, Alexandrova AN, Birch KA, Boldyrev AI, Wang LS (2003) *Angew. Chem. Int. Ed.*, 42: 6004.
20. Pei Y, Zeng XC (2008) *J. Am. Chem. Soc.* 130: 2580.
21. Aihara JI, Kanno H, Ishida T (2005) *J. Am. Chem. Soc.* 127: 13324.
22. Ricca A, Bauschlicher CW (1997) *J. Chem. Phys.*, 106: 2317.
23. (a) Curtiss LA, Pople JA (1989) *J. Chem. Phys.*, 91: 4809; (b) Lee DY, Martin JC, (1984) *J. Am. Chem. Soc.* 106: 5745-5746.
24. Yu HL, Sang RL, Wu YY (2009) *J. Phys. Chem. A* 113: 3382–3386.
25. Kalita AJ, Rohman SS, Kashyap C, Ullah SS, Guha AK (2020) *Chem. Commun.* 56: 12597.
26. Krogh-Jespersen MB, Chandrasekhar J, Wuerthwein EU, Collins JB, Schleyer PvR (1980) *J. Am. Chem. Soc.* 102: 2263–2268.
27. Ebner F, Wadepohl H, Greb L (2019) *J. Am. Chem. Soc.* 141: 18009–18012.
28. Thompson EJ, Myers TW, Berben LA (2014) *Angew. Chem., Int. Ed.* 53: 14132–14134.
29. Averkiev BB, Boldyrev AI (2008) *Russ. J. Gen. Chem.* 78: 769-773.

30. (a) Alexandrova AN, Boldyrev AI, Zhai HJ, Wang LS (2006) *Coord. Chem. Rev.* 250: 2811-2866; (b) Zubarev D, Boldyrev AI (2007) *J. Comput. Chem.*, 28: 251-268.
31. Zhang CL, Xu HG, Xu HL, Zheng WJ (2021) *J. Phys. Chem. A*, 125: 302–307.
32. Wang M, Chen C, Pan S, Cui Z (2021) *Chem. Sci.* 12: 15067-15076.
33. Zhang J, Dolg M (2015) *Phys. Chem. Chem. Phys.*, 17: 24173-24181.
34. Zhang J, Dolg M (2016) *Phys. Chem. Chem. Phys.*, 18: 3003-3010.
35. Zhao Y, Truhlar DG (2008) *Theor. Chem. Acc.*120: 215.
36. Gaussian 16, Revision B.01, Frisch MJ, Trucks GW, Schlegel HB, Scuseria GE, Robb NA, Cheeseman JR, Scalmani G, Barone V, Petersson GA, Nakatsuji H, Li X, Caricato M, Marenich AV, Bloino J, Janesko BG, Gomperts R, Mennucci B, Hratchian HP, Ortiz JV, Izmaylov AF, Sonnenberg JL, Williams-Young D, Ding F, Lipparini F, Egidi F, Goings J, Peng B, Petrone A, Henderson T, Ranasinghe D, Zakrzewski VG, Gao J, Rega N, Zheng G, Liang W, Hada M, Ehara M, Toyota K, Fukuda R, Hasegawa J, Ishida M, Nakajima T, Honda Y, Kitao O, Nakai H, Vreven Y, Throssell K, Montgomery JA, Jr., Peralta JE, Ogliaro F, Bearpark MJ, Heyd JJ, Brothers EN, Kudin KN, Staroverov VN, Keith TA, Kobayashi R, Normand J, Raghavachari K, Rendell AP, Burant JC, Iyengar SS, Tomasi J, Cossi M, Millam JM, Klene M, Adamo C, Cammi R, Ochterski JW, Martin RL, Morokuma K, Farkas O, Foresman JB and Fox DJ (2016) Gaussian, Inc., Wallingford CT.
37. Reed AE, Weinhold F, Curtiss LA (1998) *Chem. Rev.* 88: 899-926.
38. (a) Mitoraj MP, Michalak A, Ziegler TA (2009) *J. Chem. Theory Comput.*, 5: 962–975; (b) Mitoraj MP, Michalak A (2007) *J. mol. model.* 13: 347-355.
39. Zubarev DY, Boldyrev AI (2008) *Phys. Chem. Chem. Phys.* 10: 5207–5217.
40. Bader RFW (1990), Oxford Univ. Press, Oxford.
41. (a) Silvi B, Savin A (1994) *Nature*, 371: 683-686; (b)) Becke AD, Edgecombe KE (1990) *J. Chem. Phys.* 92: 5397-5403.
42. Lu T, Chen F (2012) *J. Comput. Chem.* 33: 580.
43. Schleyer PvR, Maerker C, Dransfeld A, Jiao H, Hommes NJRvE (1996) *J. Am. Chem. Soc.*, 118: 6317-6318.

Figures

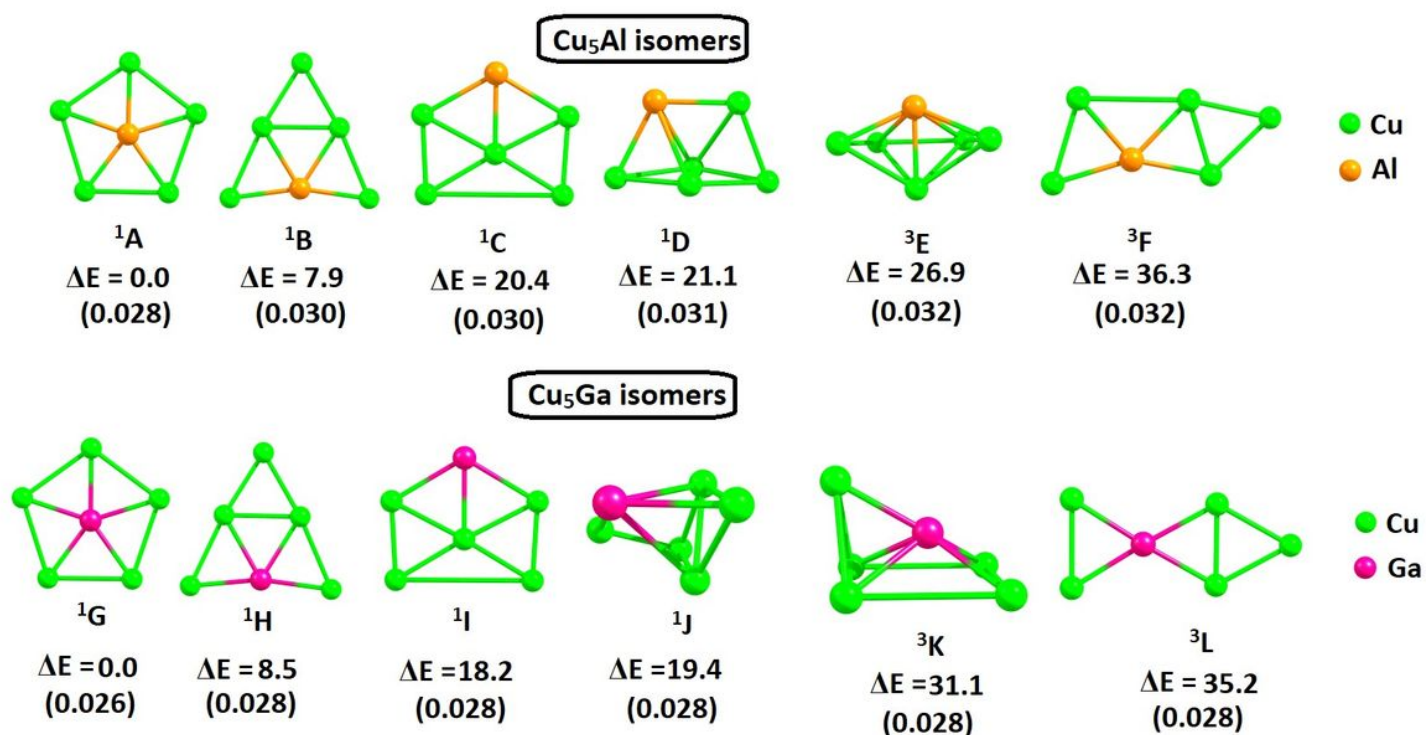
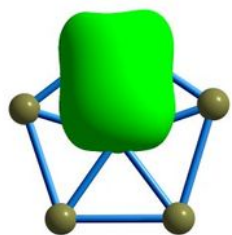
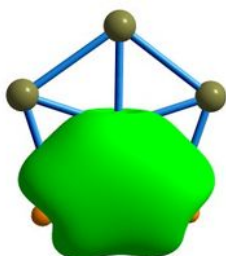


Figure 1

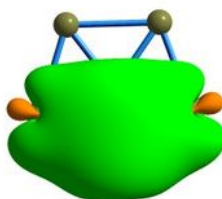
The relative energies in kcal/mol of the low energy isomers (A-L) of Cu₅Al²⁺ (top) and Cu₅Ga²⁺ (bottom) calculated at CCSD(T)/def2-TZVP//M06-2X/def2-TZVP level of theory. T_1 diagnostic values are given within parenthesis.



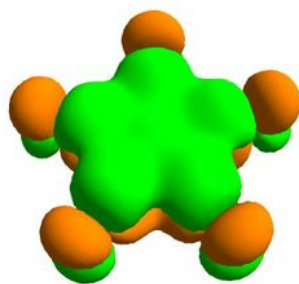
5 X 2c-2e
Cu-Al (σ)
ON = 1.99 e



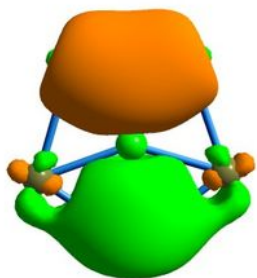
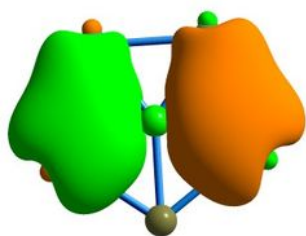
5 X 3c-2e
Cu-Al (σ)
ON = 1.99 e



5 X 4c-2e
Cu-Al (σ)
ON = 1.99 e



6c-2e
Cu-Al (π)
ON = 1.99 e



3 X 6c-2e
Cu-Al (σ)
ON = 1.99 e

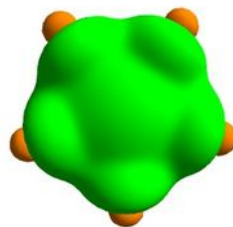


Figure 2

Bonds recovered using AdNDP analysis of $\text{Cu}_5\text{Al}^{2+}$ cluster.

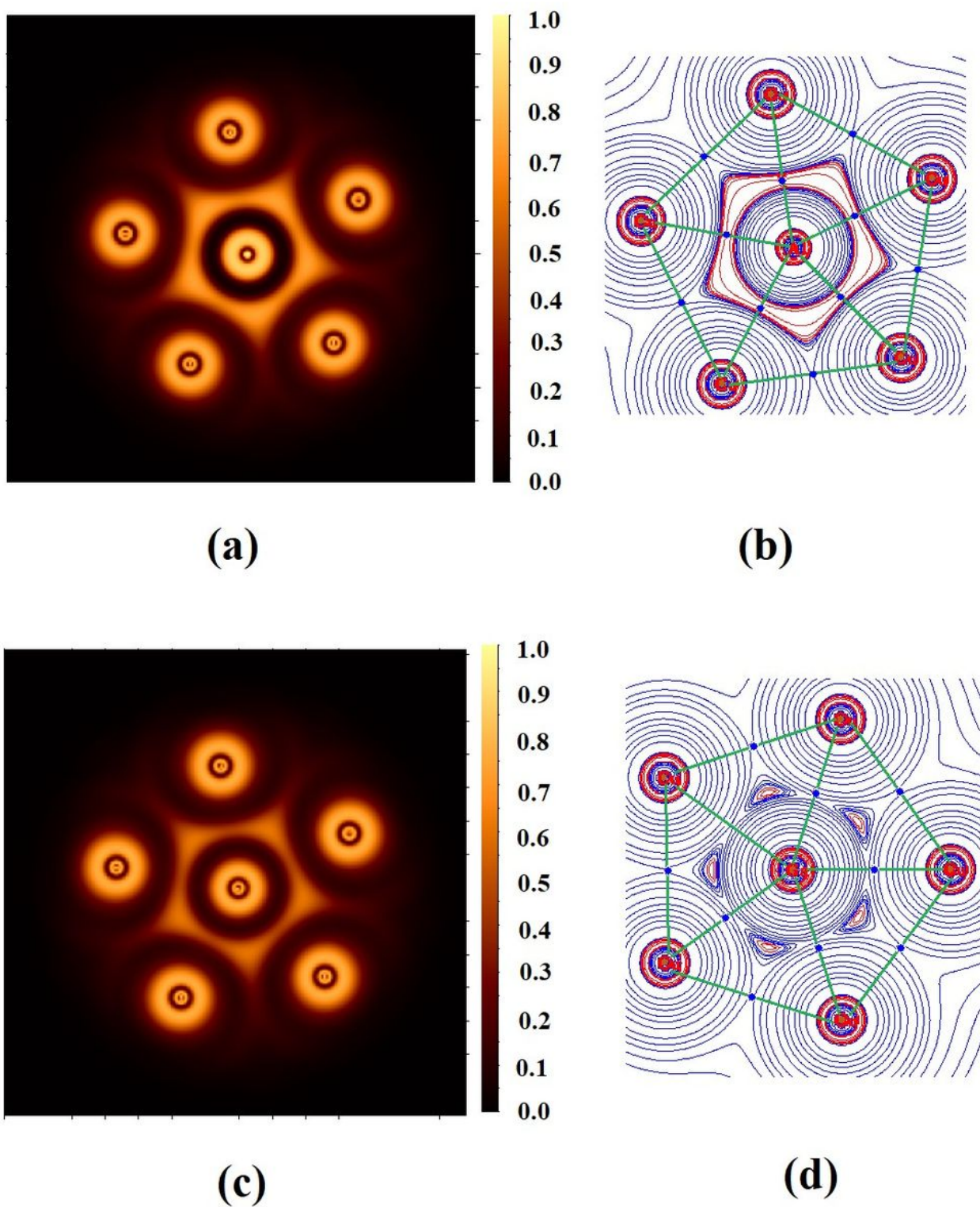


Figure 3

Plot of (a) laplacian of electron density (red = charge concentration, blue = charge depletion) and (b) electron localization function (ELF) in the molecular plane of $\text{Cu}_5\text{Al}^{2+}$ and (c) and (d) are for $\text{Cu}_5\text{Ga}^{2+}$.

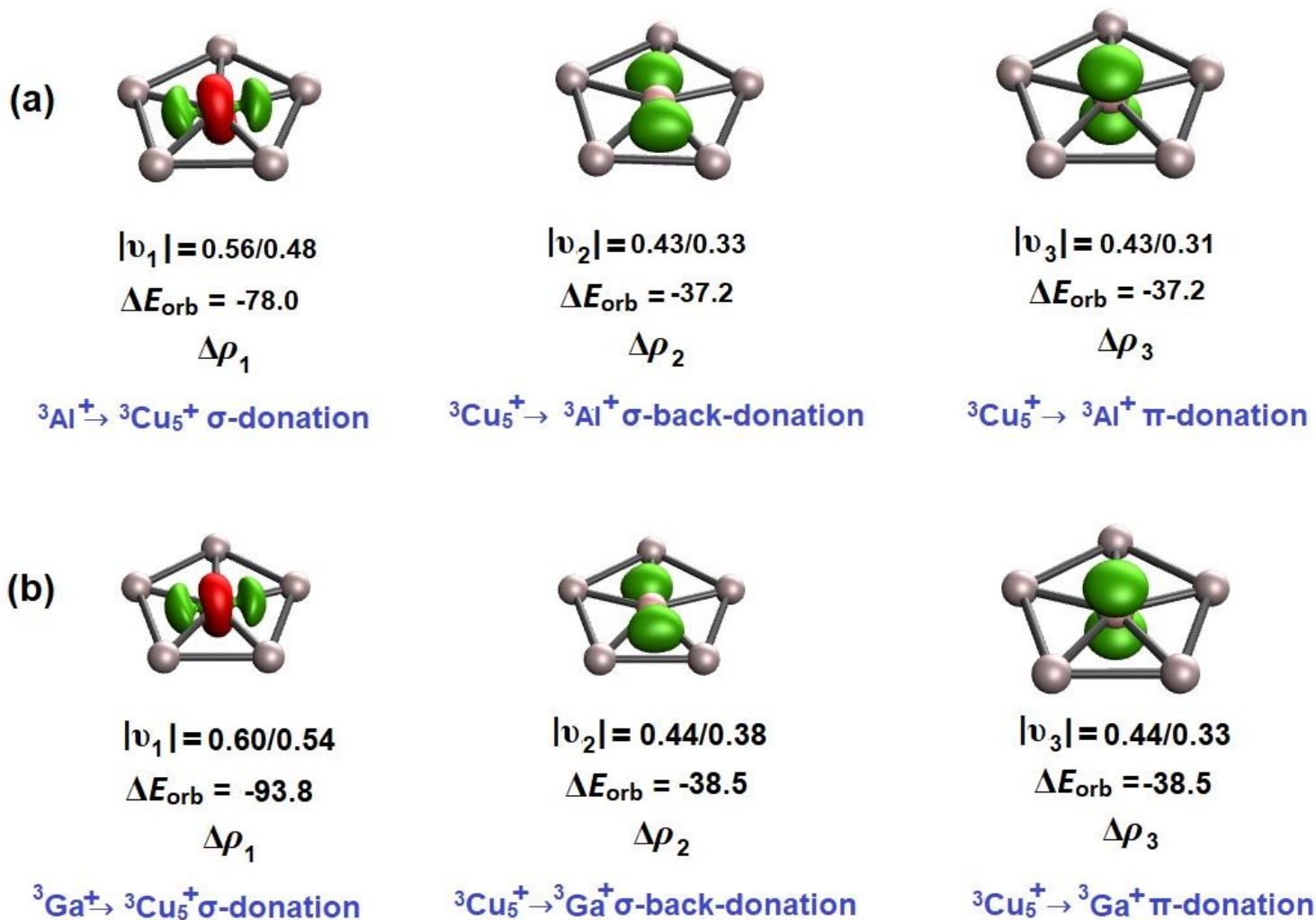


Figure 4

Plot of deformation density, $\Delta\rho$ obtained from ETS-NOCV analysis using Al^+ and Ga^+ (triplet) and Cu_5^+ in triplet state for (a) $\text{Cu}_5\text{Al}^{2+}$ and (b) $\text{Cu}_5\text{Ga}^{2+}$ clusters. Orbital values are given in kcal/mol. $|v|$ represents the (alpha/beta) charge eigenvalues. The direction of charge flow is red \rightarrow green. Cut-off employed, $\Delta\rho = 0.004$.

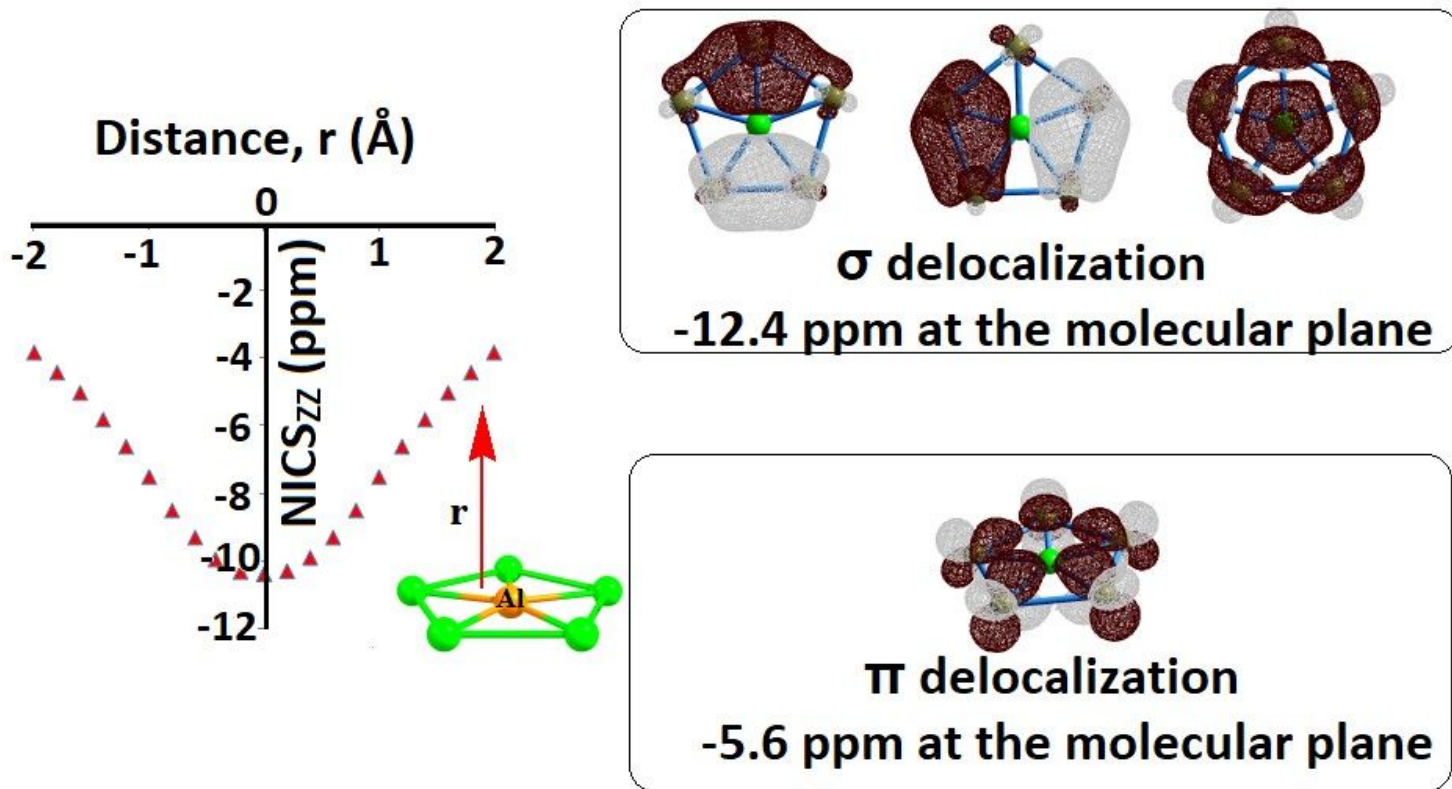
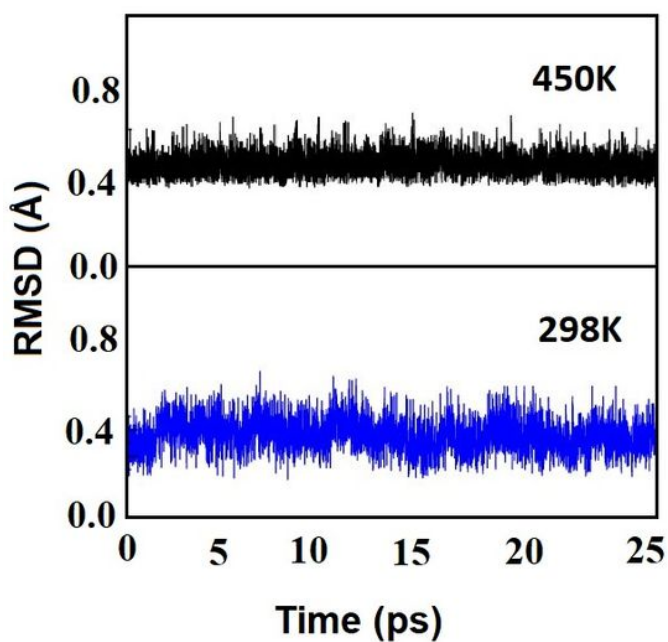
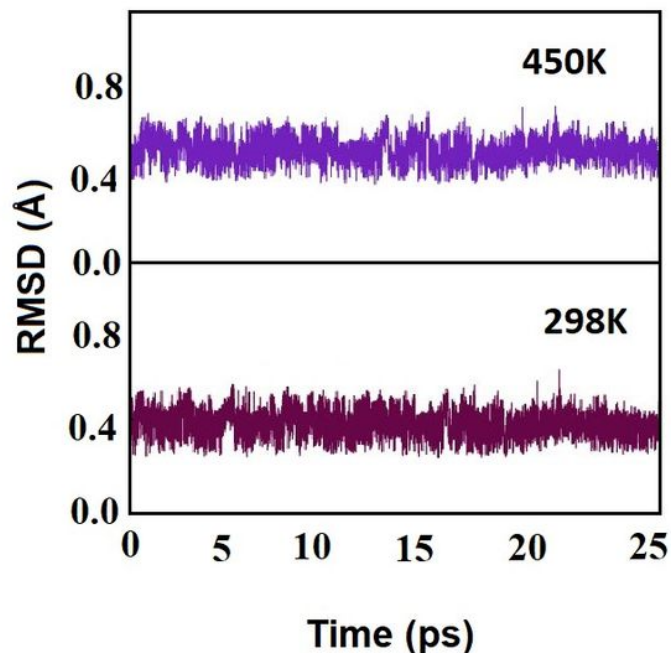


Figure 5

NICS_{ZZ} (ppm) against the perpendicular distance (Å) from the centre of the Cu-Al-Cu in Cu₅Al²⁺ cluster along with the canonical molecular orbitals (CMO) showing σ and π delocalization and their contribution to NICS_{ZZ} in the molecular plane.



(a)



(b)

Figure 6

Plot of RMSD (Å) versus time (ps) obtained from BOMD simulation (M06-2X/TZVP) at 298K and 450K for (a) $\text{Cu}_5\text{Al}^{2+}$ and (b) $\text{Cu}_5\text{Ga}^{2+}$ clusters.

Supplementary Files

This is a list of supplementary files associated with this preprint. Click to download.

- [SIAIGa.doc](#)